Testing Landscape Theory for Biomolecular Processes with Single Molecule Fluorescence Spectroscopy

Katherine Truex,* Hoi Sung Chung, John M. Louis, and William A. Eaton†
Laboratory of Chemical Physics, National Institute of Diabetes and Digestive and Kidney Diseases, National Institutes of Health (NIH), Bethesda, Maryland 20892-0520, USA
(Received 16 December 2014; published 1 July 2015)

Although Kramers' theory for diffusive barrier crossing on a 1D free energy profile plays a central role in landscape theory for complex biomolecular processes, it has not yet been rigorously tested by experiment. Here we test this 1D diffusion scenario with single molecule fluorescence measurements of DNA hairpin folding. We find an upper bound of 2.5 μs for the average transition path time, consistent with the predictions by theory with parameters determined from optical tweezer measurements.

DOI: 10.1103/PhysRevLett.115.018101 PACS numbers: 87.15.Cc, 82.37.Np, 82.39.Rt, 87.80.Nj

Introduction.—The most frequently used theoretical description for the self-assembly of biological macromolecules, such as the folding of a protein or a nucleic acid, employs what has come to be known as landscape theory. According to this theory, the kinetics of folding is described by diffusion on a low-dimensional free energy surface. Most often only a one-dimensional surface is employed with an order parameter as the reaction coordinate. In this case, the mean first passage time (the inverse of the rate coefficient) for the transition from the unfolded to the folded state is calculated from the celebrated equation of Kramers for the escape of a Brownian particle from a well over a harmonic barrier separating states [1],

$$t_{\mathrm{MFP}} = 2\pi\left(\beta D^{*}\sqrt{k_w k_b}\right)^{-1}\exp(\beta\Delta G^{*}), \qquad (1)$$

where $\beta = 1/k_B T$, D^* is the diffusion coefficient at the free energy barrier top, k_w and k_b are the stiffness (curvatures) of the free energy surface in the well and at the barrier top, respectively, and ΔG^* is the free energy barrier height [Figure 1(a)]. Although this simple one-dimensional diffusion scenario described by Eq. (1) is widely used in experimental, theoretical, and computational studies of protein and nucleic acid self-assembly and other complex biomolecular processes [3–16], it has not yet been rigorously tested by experiments.

An important quantitative test of this 1D diffusion scenario that uses no adjustable parameters is now possible due to advances in single molecule force and fluorescence spectroscopies. The first step consists of determining the 1D free energy surface from constant-force optical tweezer measurements [17–22], which yields k_w, k_b, and ΔG^*, and using the values of these parameters together with the measured t_{MFP} to obtain D^*. With these parameters it is possible to calculate a new experimental measurable, the average transition path time, which can be compared with the value determined from single molecule Förster resonance energy transfer (FRET) measurements [2,23]. The transition path time is the tiny fraction of an equilibrium trajectory when the barrier crossing actually happens, producing a jump in the experimental observable (Fig. 1), and contains all of the mechanistic information on how the molecule self-assembles. Szabo showed that the mean transition path time (t_{TP}) is given by

$$t_{\mathrm{TP}} \approx (\beta D^{*} k_b)^{-1}\ln(2e^{\gamma}\beta\Delta G^{*}), \qquad (2)$$

where γ is Euler's constant (=0.577…) [24–26].

Using the parameters determined from long trajectories containing thousands of folding and unfolding transitions in constant-force optical tweezer experiments on DNA hairpins, Woodside and co-workers [18,27] calculated transition path times from Eq. (2). However, they could not directly measure them, because they were all less than 50 μs, the time resolution of their instrument. In this work, we take advantage of the much better time resolution of single molecule fluorescence measurements. We use the single molecule FRET method and compare our results for the mean transition path time of a DNA hairpin (Fig. 2) with the time predicted for this hairpin by Woodside and co-workers and a theoretical prediction on how the

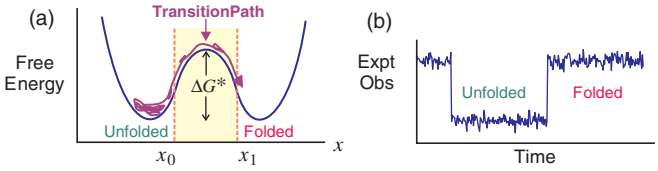

FIG. 1 (color). (a) A one-dimensional free energy surface (blue curve) for folding with x as the reaction coordinate (from Ref. [2]). The transition path is the rare segment of the folding trajectory during which there is a successful crossing of the barrier between the unfolded and folded states and is defined as a trajectory which crosses x_0 and reaches x_1 on the other side of the barrier without recrossing x_0 (violet curve). (b) Trajectory of an experimental observable, such as the FRET efficiency in single molecule fluorescence experiments or molecular extension in constant-force optical tweezer experiments, illustrating that in experiments the transition path appears as a nearly instantaneous jump.

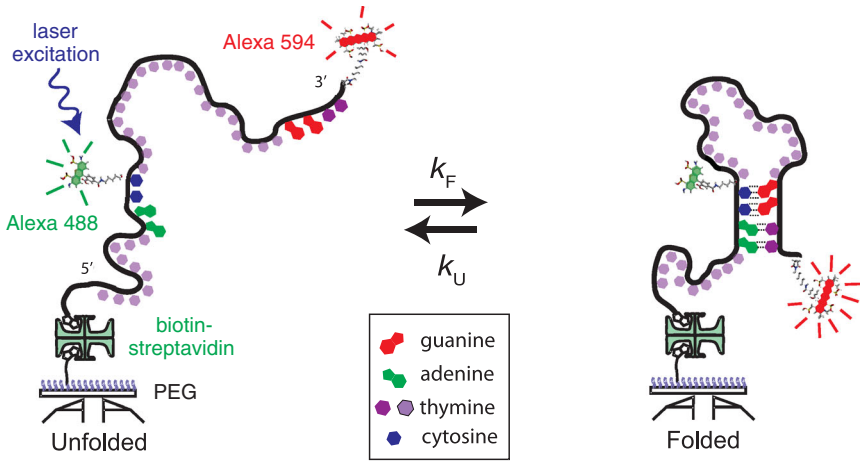

FIG. 2 (color). Schematic diagram of the single-stranded DNA construct [5′-AACC(T_{21})GGTT − 3′] in an unfolded and a hairpin-folded conformation with fluorescent dye labels and immobilized on a polyethylene glycol coated coverslip via a biotin-streptavidin-biotin linkage. k_F and k_U are the folding and unfolding rate coefficients. The 2 thymines that form base pairs in the folded hairpin are distinguished by a darker purple color.

transition path time depends on stem length by Frederickx *et al.*, based on a polymer physics model [28].

Experimental results.—The ideal comparison would be to study the same DNA hairpins used in the force experiments. However, that is not yet possible because their high stability and low transition frequency make them inaccessible to single molecule FRET measurements, which require folding and unfolding times on the millisecond time scale or less for acquiring data before fluorophore bleaching at the necessarily high illumination intensities terminates the photon trajectories. The DNA hairpin employed in our study has a stem of four base pairs with a flexible loop consisting of 21 thymines (Fig. 2). This hairpin was selected because the loop is sufficiently long to result in a significantly lower FRET efficiency in the unfolded, compared to the folded, state and because the several hundred microsecond folding and unfolding times [29,30] are sufficiently short for the acquisition of many transitions. In addition, analysis of the photon trajectories is much simplified by the fact that this hairpin behaves like a two-state system, i.e., a system with only folded and unfolded populations detectable at equilibrium and at all times in kinetic experiments.

Single molecule fluorescence measurements were made using a confocal microscope system [31]. Initial measurements carried out at power densities of ~2 kW/cm^2 resulted in an average detection rate of 120 photons/ms and produced photon trajectories that were long enough to observe multiple folding and unfolding transitions prior to bleaching of either the donor or acceptor fluorophore. The transition frequency, however, was too high to obtain waiting time distributions for the determination of rate coefficients from FRET efficiency [$E = n_{\text{acceptor}}/(n_{\text{acceptor}} + n_{\text{donor}})$] trajectories. Instead, precise rate coefficients were determined from a photon-by-photon analysis of the trajectories using the maximum likelihood method of Gopich and Szabo [24,37]. By maximizing a likelihood function, their method yields the parameters of an assumed model that are most consistent with the photon trajectories consisting of colors (donor or acceptor) and intervals between detected photons. The likelihood function for the jth trajectory consisting of N photons is

$$L_j = \mathbf{1}^{\mathrm{T}} \prod_{i=2}^{N} \{\mathbf{F}(c_i) \exp[\mathbf{K}\tau_i]\} \mathbf{F}(c_1)\, \mathbf{p}_{\text{eq}}, \tag{3}$$

where c_i is the color of the ith photon in the trajectory, τ_i is the time interval between the ith and the (i-1)th photon, $\mathbf{F}$ is the photon color matrix where $\mathbf{F}(\text{acceptor}) = \mathbf{E}$ and $\mathbf{F}(\text{donor}) = \mathbf{I} - \mathbf{E}$, $\mathbf{E}$ is a diagonal matrix of the FRET efficiencies of the states, $\mathbf{I}$ is the identity matrix, $\mathbf{K}$ is the rate matrix that depends on the specific model, $\mathbf{p}_{\text{eq}}$ is a column vector that gives the equilibrium populations of folded and unfolded states, and $\mathbf{1}^{\mathrm{T}}$ is the row vector (1 1) for a two-state system. This form of the likelihood function is valid if the total (acceptor plus donor) photon count rate is approximately the same in each state, as is the case in our experiments. The two-state rate matrix is $\mathbf{K}_{2\text{-state}} = \begin{pmatrix} -k_{\mathrm{U}} & k_{\mathrm{F}} \\ k_{\mathrm{U}} & -k_{\mathrm{F}} \end{pmatrix}$. The rate coefficients and FRET efficiencies that resulted from applying Eq. (3) to 200 photon trajectories with an average length of 60 ms and an average count rate of 120 photons/ms are given in Table SI [31].

The adequacy of the two-state model was confirmed using several criteria. First, 50 μs binning of the data collected at high illumination intensity shows only 2 peaks, corresponding to folded and unfolded states, with widths accounted for by shot noise [Fig. 3(d)]. In addition, the histogram constructed from 1 ms binning at the lower intensity (120 photons/ms) used for determining rate coefficients is nearly identical to the histogram constructed by re-coloring the trajectories assuming a two-state model (Supplemental Material, Fig. S2, [31]) [24,37]. Finally,

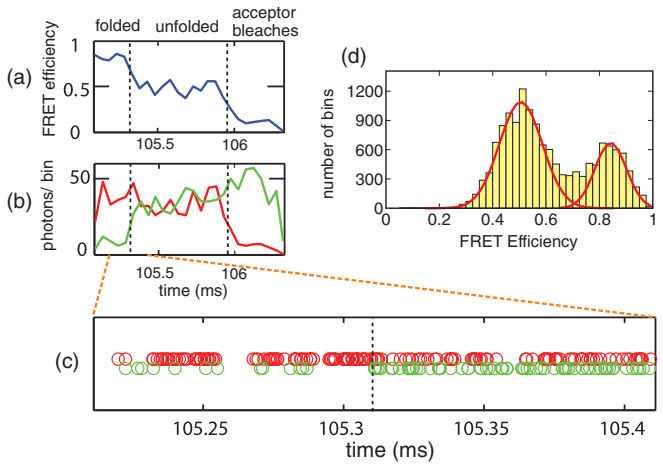

FIG. 3 (color). Representative single molecule FRET data for an immobilized DNA hairpin at high power density (20 kW/cm^2 and an average count rate of 870 photons/ms). (a) FRET efficiency trajectory. FRET efficiency was calculated for photons collected in 50 μs bins (b) Trajectories of donor (green) and acceptor (red) fluorescence (50 μs bins). (c) Photon trajectory. Each circle represents a detected photon. Red circles (upper row) are acceptor photons. Green circles (lower row) are donor photons. The dashed line indicates a transition predicted by the Viterbi algorithm [38,39]. (d) FRET efficiency histogram (power density of 20 kW/cm^2; 870 detected photons/ms) calculated from photons in 50 μs bins [40]. The continuous red curves are Gaussian fits to the 2 peaks of the histogram using the width expected from shot noise. Intermediate values of the FRET efficiency contribute to the histogram, because ~15% of the bins used to construct the histogram contain a transition between the folded and unfolded states.

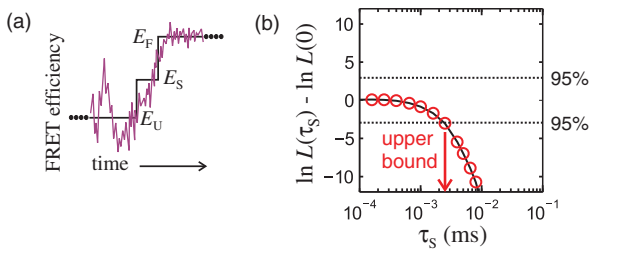

FIG. 4 (color). Kinetic model and maximum likelihood analysis of photon trajectories. (a) The noisy curve is a schematic of the instantaneous FRET for a transition path from the unfolded to folded states. The step curve is the simplest discretization of the path with average FRET efficiencies E_U for the unfolded state, E_F for the folded state, and an intermediate value $E_S = (E_U + E_F)/2$ for the virtual step state. (b) Comparison of the values of the likelihood function from the three state analysis, $L(\tau_S)$, and a two-state analysis with an instantaneous transition, $L(0)$, calculated for 780 transitions from immobilized molecules. The result of the calculation is that no lifetime greater than 2.5 μs is detected by the measurement, so the average transition path time is shorter than 2.5 μs. Acceptor blinking can interfere with the transition path time analysis [42], but was effectively eliminated by not including transitions in which there are nearby strings of 8 or more donor photons [31].

the decay rate of 3.7 ms^{-1} for the donor-acceptor cross-correlation function, which is a totally independent analysis of the immobilization data [41], is close to the sum of the rate coefficients of 5.1 ms^{-1} (Supplemental Material, Fig. S3, [31]) from the maximum likelihood analysis, the difference being readily explained by donor blinking [42].

As in previous studies [2,23], to analyze trajectories at high illumination intensity [Figs. 3(a), 3(b), and 3(c)] for transition path time measurements, we employed a model consisting of the simplest discretization of a transition path, with a single virtual "step" state treated as a kinetic intermediate having a FRET efficiency midway between the folded and unfolded states (Fig. 4). The average time spent between the folded and unfolded states during the transition path—the lifetime of this step state ($\tau_S = 1/2k_S$)—is therefore identified as the average transition path time. This simplification allowed us to use a 3-state kinetic model for calculating the value of the likelihood function. The rate matrix $\mathbf{K}$ of Eq. (3) now becomes

$$\mathbf{K}_{\text{3-state}} = \begin{pmatrix} -k_{U'} & k_S & 0 \\ k_{U'} & -2k_S & k_{F'} \\ 0 & k_S & -k_{F'} \end{pmatrix}, \qquad (4)$$

where $k_{U'}$ and $k_{F'}$ are related to parameters known from the low intensity experiments (see [31] and parameters in Table SI), so only a single parameter, k_S, the rapid rate from the step state to the folded or unfolded state, needs to be varied to maximize the likelihood function. The values of the likelihood function for each trajectory were computed as described in Ref. [2] with unique values of E_F, E_U, and E_S for each trajectory, since the local environment of each molecule immobilized on the glass slightly affects its FRET efficiency. The total log-likelihood for a data set of n transitions is given by $\ln L = \sum_{m=1}^{n} \ln L_m$. The likelihood function for the mth segment containing a single transition is given by Eq. (3), but with $\mathbf{p}_{\text{eq}}$ replaced by $\mathbf{v}_{\text{initial}}$ and $\mathbf{1}^{\text{T}}$ replaced by $\mathbf{v}_{\text{final}}$, since the initial and final states are known.

Figure 4(b) shows the difference in the values of the log-likelihood functions, $\Delta \ln L = \ln L(\tau_S) - \ln L(0)$, where the likelihood function, L, is for the three-state model as described above for 780 transitions between folded and unfolded states. $L(0)$ represents the case for an instantaneous transition between the folded and unfolded states in a two-state model. Thus, the plot shows whether a three-state model with a finite transition path time or a two-state model with an instantaneous transition is more likely by comparing the values of the likelihood function for each model. The dashed horizontal lines correspond to the 95% confidence levels defined by $L(\tau_S)/[L(\tau_S) + L(0)] = 0.95$ or $L(0)/[L(\tau_S) + L(0)] = 0.95$. For a given value of τ_S, $\Delta \ln L = 0$ indicates that both models are equally consistent with the data, while values of $\Delta \ln L > 0$ indicate that the three-state model is more likely and the value of τ_S at a peak in $\Delta \ln L > 3$ corresponds to the average transition path time [2,23]. When no peak is observed, the value of τ_S at $\Delta \ln L = -3$ indicates with 95% confidence that an instantaneous model is more consistent with the data and

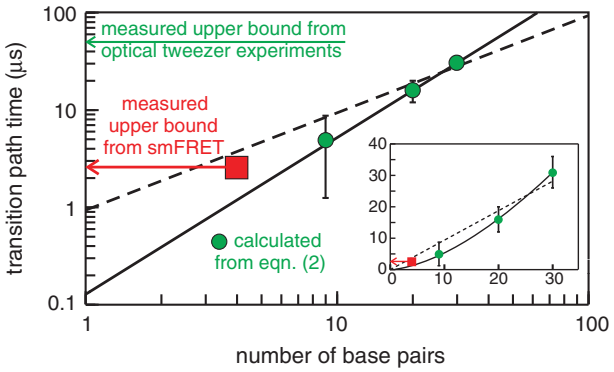

FIG. 5 (color). Transition path time as a function of the number of base pairs in the stem of the folded structure. The green circles with error bars were calculated from Eq. (2) by Neupane *et al.* [18] from force spectroscopic determinations of ΔG^*, D^*, and k_b for DNA hairpins with stem lengths of 20 and 30 base pairs and a DNA aptamer with a stem of 9 base pairs. The red square with an arrow attached is the upper bound of 2.5 μs determined in this work for the 4-base-pair stem of the DNA hairpin using single molecule FRET. The broken curve is from Neupane *et al.*, which assumes that $t_{TP} \sim N$, while the continuous curve is $t_{TP} \sim N^{\alpha}$ with $\alpha = 1.6$ from Frederickx *et al.* [28]. Inset is the same points and curves on a linear scale.

that there is no lifetime detected in the trajectories longer than this value [2]. For our data $\Delta \ln L = -3$ when $\tau_S = 2.5$ μs, which is therefore an upper bound for the average transition path time. Recoloring the same set of trajectories for several fixed values of τ_S demonstrates that for the number of observed transitions, photon count rate, and FRET efficiencies in our experiments no significant peaks could possibly be observed for $t_{TP} \lesssim 5$ μs.

Discussion.—Our determination of 2.5 μs for the upper bound for the average transition path time of this DNA hairpin represents a major improvement in time resolution compared with the 50 μs upper bound that could be obtained in the force spectroscopic experiments [18]. A comparison of our experimental result with the predictions from the optical tweezer experiments based on Eq. (2) (Fig. 5) raise interesting and important issues. To explain the predicted dependence of the average transition path time (t_{TP}) on the number of base pairs in the stem (N) (Fig. 5) Woodside and co-workers made the assumption that $t_{TP} \sim N$ [18]. On the other hand, Frederickx *et al.* developed a theoretical model for the transition path time at zero force, confirmed by coarse-grained simulations, that yielded a power law, $t_{TP} \sim N^{\alpha}$, with $\alpha = 1 + \nu$, where $\nu = 0.59$ is the Flory exponent [28]. Their theoretical curve with a best-fit α of 1.6 ± 0.4 agrees remarkably well with the experimental data (Fig. 5). The nonlinear dependence in their theory results from a diffusion coefficient that is position dependent because of an increase in strand tension as the stem zips up.

Comparison between our measured upper bound for the transition path time and the predicted value from the parameters determined in Woodside's force measurements has several caveats, including the fact that the polythymine loop in the fluorescence measurements is much larger (21 compared to 4) and the important assumptions that both the experimentally determined diffusion coefficient and barrier-top curvature used by Woodside and co-workers in calculating the transition path times from Eq. (2) are unchanged when the force is removed. Nevertheless, the close correspondence of our upper bound of 2.5 μs, compared to the predicted values of 3.6 and 1 μs from the linear and power law fits to the force data, respectively, is a significant result, for it is one of the most convincing pieces of experimental evidence that the diffusion on a 1D free energy surface scenario may indeed provide a quantitative description of a complex self-assembly process. Another important test of the 1D scenario is currently being carried out by analyzing the all-atom molecular dynamics simulations of protein folding by the D.E. Shaw group. Comparisons of mean first passage and transition path times with those calculated from the 1D free energy surface and diffusion coefficient from the simulations using the number of native contacts as the reaction coordinate are so far in good agreement [43,44]. If both experiments and atomistic simulations show that the theory for motion of a single Brownian particle on a 1D surface does turn out to be near quantitatively perfect for folding DNA hairpins and proteins, it raises the interesting and important question of why such a simple theory works so well.

We thank Attila Szabo, Irina Gopich, and Robert Best for numerous helpful discussions. This work was supported by the Intramural Research Program of the NIDDK, NIH.

*Corresponding author.
truexkl@mail.nih.gov
†Corresponding author.
eaton@helix.nih.gov

[1] H. A. Kramers, Brownian motion in a field of force and the diffusion model of chemical reactions, Physica (Amsterdam) **7**, 284 (1940).
[2] H. S. Chung, K. McHale, J. M. Louis, and W. A. Eaton, Single-molecule fluorescence experiments determine protein folding transition path times, Science **335**, 981 (2012).
[3] J. D. Bryngelson and P. G. Wolynes, Intermediates and barrier crossing in a random energy-model (with applications to protein folding), J. Phys. Chem. **93**, 6902 (1989).
[4] C. M. Dobson, A. Sali, and M. Karplus, Protein folding: A perspective from theory and experiment, Angew. Chem. **37**, 868 (1998).
[5] P. G. Wolynes, Recent successes of the energy landscape theory of protein folding and function, Q. Rev. Biophys. **38**, 405 (2005).
[6] P. Faccioli, M. Sega, F. Pederiva, and H. Orland, Dominant Pathways in Protein Folding, Phys. Rev. Lett. **97**, 108101 (2006).
[7] R. B. Best and G. Hummer, Diffusive Model of Protein Folding Dynamics with Kramers Turnover in Rate, Phys. Rev. Lett. **96**, 228104 (2006).

[8] E. Shakhnovich, Protein folding thermodynamics and dynamics: Where physics, chemistry, and biology meet, Chem. Rev. **106**, 1559 (2006).
[9] V. Munoz, Conformational dynamics and ensembles in protein folding, Annu. Rev. Biophys. Biomol. Struct. **36**, 395 (2007).
[10] D. Thirumalai, E. P. O'Brien, G. Morrison, and C. Hyeon, Theoretical perspectives on protein folding, Annu. Rev. Biophys. **39**, 159 (2010).
[11] R. B. Best and G. Hummer, Coordinate-dependent diffusion in protein folding, Proc. Natl. Acad. Sci. U.S.A. **107**, 1088 (2010).
[12] H. S. Chan, Z. Zhang, S. Wallin, and Z. Liu, Cooperativity, local-nonlocal coupling, and nonnative interactions: principles of protein folding from coarse-grained models, Annu. Rev. Phys. Chem. **62**, 301 (2011).
[13] P. C. Whitford, K. Y. Sanbonmatsu, and J. N. Onuchic, Biomolecular dynamics: order-disorder transitions and energy landscapes, Rep. Prog. Phys. **75**, 076601 (2012).
[14] E. R. Henry, R. B. Best, and W. A. Eaton, Comparing a simple theoretical model for protein folding with all-atom molecular dynamics simulations, Proc. Natl. Acad. Sci. U.S.A. **110**, 17880 (2013).
[15] R. B. Best, G. Hummer, and W. A. Eaton, Native contacts determine protein folding mechanisms in atomistic simulations, Proc. Natl. Acad. Sci. U.S.A. **110**, 17874 (2013).
[16] H. Gelman and M. Gruebele, Fast protein folding kinetics, Q. Rev. Biophys. **47**, 95 (2014).
[17] M. T. Woodside, P. C. Anthony, W. M. Behnke-Parks, K. Larizadeh, D. Herschlag, and S. M. Block, Direct measurement of the full sequence-dependent landscape of a nucleic acid, Science **314**, 1001 (2006).
[18] K. Neupane, D. B. Ritchie, H. Yu, D. A. N. Foster, F. Wang, and M. T. Woodside, Transition Path Times for Nucleic Acid Folding Determined from Energy-Landscape Analysis of Single-Molecule Trajectories, Phys. Rev. Lett. **109**, 068102 (2012).
[19] M. Hinczewski, J. C. M. Gebhardt, M. Rief, and D. Thirumalai, From mechanical folding trajectories to intrinsic energy landscapes of biopolymers, Proc. Natl. Acad. Sci. U.S.A. **110**, 4500 (2013).
[20] M. T. Woodside and S. M. Block, Reconstructing folding energy landscapes by single-molecule force spectroscopy, Annu. Rev. Biophys. **43**, 19 (2014).
[21] M. T. Woodside, J. Lambert, and K. S. D. Beach, Determining intrachain diffusion coefficients for biopolymer dynamics from single-molecule force spectroscopy measurements, Biophys. J. **107**, 1647 (2014).
[22] M. C. Engel, D. B. Ritchie, D. A. N. Foster, K. S. D. Beach, and K. T. Woodside, Reconstructing Folding Energy Landcsape Profiles from Nonequilibrium Pulling Curves with an Inverse Weierstrass Integral Transform, Phys. Rev. Lett. **113**, 238104 (2014).
[23] H. S. Chung and W. A. Eaton, Single-molecule fluorescence probes dynamics of barrier crossing, Nature (London) **502**, 685 (2013).
[24] H. S. Chung and I. V. Gopich, Fast single-molecule FRET spectroscopy: theory and experiment, Phys. Chem. Chem. Phys. **16**, 18644 (2014).
[25] H. S. Chung, J. M. Louis, and W. A. Eaton, Experimental determination of upper bound for transition path times in protein folding from single-molecule photon-by-photon trajectories, Proc. Natl. Acad. Sci. U.S.A. **106**, 11837 (2009).
[26] S. Chaudhury and D. E. Makarov, A harmonic transition state approximation for the duration of reactive events in complex molecular rearrangements, J. Chem. Phys. **133**, 034118 (2010).
[27] G. Hummer and W. A. Eaton, Viewpoint: Transition path times for DNA and RNA folding from force spectroscopy, Physics **5**, 87 (2012).
[28] R. Frederickx, T. in't Veld, and E. Carlon, Anomalous Dynamics of DNA Hairpin Folding, Phys. Rev. Lett. **112**, 198102 (2014).
[29] J. Jung, R. Ihly, E. Scott, M. Yu, and A. Van, Orden, Probing the complete folding trajectory of a DNA hairpin using dual beam fluorescence fluctuation spectroscopy, J. Phys. Chem. B **112**, 127 (2008).
[30] R. Narayanan, L. Zhu, Y. Velmurugu, J. Roca, S. V. Kuznetsov, G. Prehna, L. J. Lapidus, and A. Ansari, Exploring the energy landscape of nucleic acid hairpins using laser temperature-jump and microfluidic mixing, J. Am. Chem. Soc. **134**, 18952 (2012).
[31] See Supplemental Material at http://link.aps.org/supplemental/10.1103/PhysRevLett.115.018101, which includes Refs. [32–36], for details on the materials, methods, and supplemental data.
[32] I. V. Gopich, Concentration effects in "single-molecule" spectroscopy, J. Phys. Chem. B **112**, 6214 (2008).
[33] J. Vogelsang, R. Kasper, C. Steinhauer, B. Person, M. Heilemann, M. Sauer, and P. Tinnefeld, A reducing and oxidizing system minimizes photobleaching and blinking of fluorescent dyes, Angew. Chem. **47**, 5465 (2008).
[34] W. Kugel, A. Muschielok, and J. Michaelis, Bayesian-inference-based fluorescence correlation spectroscopy and single-molecule burst analysis reveal the influence of dye selection on DNA hairpin dynamics, ChemPhysChem **13**, 1013 (2012).
[35] M. Orrit, Chemical and physical aspects of charge transfer in the fluorescence intermittency of single molecules and quantum dots, Photochem. Photobiol. Sci. **9**, 637 (2010).
[36] T. Cordes, J. Vogelsang, and P. Tinnefeld, On the mechanism of trolox as antiblinking and antibleaching reagent, J. Am. Chem. Soc. **131**, 5018 (2009).
[37] I. V. Gopich and A. Szabo, Decoding the pattern of photon colors in single-molecule FRET, J. Phys. Chem. B **113**, 10965 (2009).
[38] L. R. Rabiner, A tutorial on hidden Markov models and selected applications in speech, Proc. IEEE **77**, 257 (1989).
[39] A. J. Viterbi, Error bounds for convolution codes and an asymptotically optimum decoding algorithm, IEEE Trans. Inf. Theory **13**, 260 (1967).
[40] I. V. Gopich and A. Szabo, Theory of single-molecule FRET efficiency histograms, in *Single-Molecule Biophysics: Experiment and Theory* I. V. Gopich and A. Szabo (John Wiley & Sons, Inc., Hoboken, 2011), 146.
[41] H. S. Chung, I. V. Gopich, K. McHale, T. Cellmer, J. M. Louis, and W. A. Eaton, Extracting rate coefficients from single-molecule photon trajectories and FRET efficiency histograms for a fast-folding protein, J. Phys. Chem. A **115**, 3642 (2011).
[42] H. S. Chung, T. Cellmer, J. M. Louis, and W. A. Eaton, Measuring ultrafast protein folding rates from photon-by-photon analysis of single molecule fluorescence trajectories, Chem. Phys. **422**, 229 (2013).
[43] H. S. Chung, S. Piana, D. E. Shaw, and W. A. Eaton (unpublished).
[44] W. Zheng and R. B. Best (unpublished).